Effects of Solubilized Water on the Relaxation Dynamics Surrounding 6-Propionyl-2-(*N*,*N*-dimethylamino)naphthalene Dissolved in 1-Butyl-3-methylimidazolium Hexafluorophosphate at 298 K

Sheila N. Baker,[§] Gary A. Baker,[||] Chase A. Munson,[†] Fei Chen,[‡] Eric J. Bukowski,[†] Alexander N. Cartwright,[‡] and Frank V. Bright*[,†]

Department of Chemistry, Natural Sciences Complex, and Department of Electrical Engineering, Bonner Hall, University at Buffalo, The State University of New York, Buffalo, New York 14260-3000

We report on the picosecond time-resolved fluorescence of 6-propionyl-2-(*N*,*N*-dimethylamino)-naphthalene (PRODAN) dissolved in 1-butyl-3-methylimidazolium hexafluorophosphate ([bmim]-[PF_6]) at 298 K as a function of solubilized water in the [bmim][PF_6] phase. The observed solvent relaxation dynamics can be described by three components with apparent relaxation times that occur over a large time regime (<15 ps to >10 ns). The average relaxation dynamics become faster as the water concentration in the [bmim][PF_6] phase increases. Libration and vibration, ion ballistic motion, ion local basin exploration, and ion basin hopping, ion diffusion, and/or the ultrafast relaxation from water (or other small molecules/impurities) are suggested as possible reasons for the yet unquantified sub-15-ps dynamics. The sub-nanosecond dynamics are consistent with [PF_6] anion relaxation. This process was found to be water-dependent, slowing as the amount of solubilized water in the [bmim][PF_6] phase increased. We speculate that this slowing arises from the formation of 1:2 H-bonded [PF_6]···HOH···[PF_6] complexes. The nanosecond dynamics are consistent with the cation, decreasing slightly with an increase in the amount of solubilized water. We suggest that the decrease in this relaxation time arises from a decrease in the bulk viscosity on adding water.

Introduction

The unique properties of room-temperature ionic liquids (RTILs) have led to their use as environmentally responsible solvents.[1−6] Given their wide utility, it should not be surprising to learn that RTILs are being investigated as alternatives to volatile organic solvents in several industrial processes and larger scale separations.[7−10] However, despite their growing use, we await a complete molecular-level picture of solute solvation in pure RTILs and liquid/RTIL mixtures. Although numerous papers have appeared on the topic of solute solvation in RTILs,[11−20] most have focused on *static* aspects of solute solvation. Despite its importance, only a limited number of experimental[21−27] and theoretical[28,29] reports have appeared on *time-dependent* solvation in ionic liquids. In fact, only a handful of reports have appeared on time-dependent solvation in RTILs near room temperature[24−29] and there have not been any time-dependent solvation studies on liquid/RTIL mixtures.

When a dipolar solvent, at equilibrium with a dissolved solute, is perturbed locally by an instantaneous change in the solute's dipole moment (as would occur during solute optical excitation), there will ensue a time-dependent re-equilibration/reorientation of the solvent molecules around the solute's newly created charge distribution. This time-dependent re-equilibration of solvent molecules is referred to as solvent relaxation/reorganization.[30−34] If the solute is fluorescent, solvent relaxation can manifest itself as a time-dependent shift in the solute's fluorescence spectrum. Thus, by recording time-resolved fluorescence intensity decay data across the solute's emission spectrum, one can assess the time course of solvation. This approach has been used previously to study "solvation" dynamics in pure liquids, liquid mixtures, electrolyte solutions, micelles, emulsions, vesicles, lipid bilayers, sol−gel-derived xerogels, cyclodextrins, and biomolecules.[33,34]

Solvent relaxation experiments have been reported previously in pure ionic liquids.[21−26] For example, Huppert and co-workers reported on the time-resolved fluorescence of coumarin 153, coumarin 102, and 6-(*N*-(4-methylphenyl)amino]-2-naphthalene-*N*,*N*-dimethyl-sulfonamide dissolved in molten tetraalkylammonium ionic liquids above 373 K.[21−23] The authors reported that their spectral shift correlation function could be described by two discrete relaxation times. The two recovered time constants were assigned to cation and anion translational motions, and both terms depended on the cation size. The instrument response time for these experiments was ∼55 ps. As a result, faster dynamics were not observed nor was the magnitude of any such fast component(s), if any, to the fully spectral shift correlation function, estimated. Karmakar and Samanta[24,25] reported on the solvent relaxation surrounding coumarin 153 and 6-propionyl-2-(*N*,*N*-dimethylamino)naphthalene (PRODAN) dissolved in 1-butyl-

* To whom correspondence should be addressed. Tel: 716-645-6800 ext. 2162. Fax: 716-645-6963. E-mail: chefvb@acsu.buffalo.edu.

[†] Department of Chemistry.

[‡] Department of Electrical Engineering.

[§] Current address: Chemical Science and Technology Division, Los Alamos National Laboratory, Los Alamos, NM 87545.

[||] Current address: Michelson Resource, Bioscience Division, Los Alamos National Laboratory, Los Alamos, NM 87545.

10.1021/ie0303606 CCC: $25.00
Published on Web 09/16/2003

3-methylimidazolium tetrafluoroborate, [bmim][BF_4], and 1-ethyl-3-methylimidazolium tetrafluoroborate, [emim][BF_4], at 293 K. The solvent relaxation kinetics in these RTILs were described by two relaxation processes. The faster of the recovered relaxation times was assigned to the anion. The slower relaxation time was assigned to collective cation and anion diffusion. These authors also showed that more than 50% of the total solvent relaxation dynamics occurred on a time scale below 50 ps (their instrument time resolution). More recently, Maroncelli and co-workers[26] reported the solvation dynamics of 4-aminophthalimide (4-AP) dissolved in 1-butyl-3-methylimidazolium hexafluorophosphate, [bmim][PF_6], between 298 and 355 K. These authors showed that dynamics occurred on two distinct time scales: (1) a very rapid, unquantified component (<5 ps) that was responsible for about half the dynamics and (2) slower dynamics taking place in the 100 ps to 10 ns regime.

There have also been molecular dynamics studies on [bmim][PF_6],[28,29] the most widely studied RTIL. The Berne group[28] computed the time-dependent mean square center of mass displacement of the [bmim] and [PF_6] ions at 303 K between 0 and 40 ps. The results of these simulations showed that there are three time scales: [1] a fast 3−4 ps process, [2] a nonlinear intermediate event, and [3] diffusive linear behavior after ∼15 ps. The short time process was assigned to ion ballistic motion on a femtosecond time scale *and* ion local basin exploration on the low picosecond time scale. The intermediate time regime was assigned to ion basin hopping. The longer time term was ascribed to ion diffusion. In related work, Morrow and Maginn[29] reported molecular dynamics studies on [bmim][PF_6] at 298 K between 0 and 2.8 ns. Their "cage correlation function" was described by [1] a rapid decay at short times (<0.5 ns) assigned to ion vibrational motion near a cage edge, [2] a plateau, and [3] a 1.5 ns time constant assigned to the average time for any ion to leave another ion's vicinity. Taken together, the aforementioned experiments and simulations show that the solvation dynamics in RTILs are [1] multimodal and [2] they occur over a remarkably wide time window (femtoseconds to nanoseconds).

The presence of small amounts of water are known to affect a RTIL's viscosity, density, conductivity, and solvent capacity[35−39] and trace amounts of water in a RTIL can alter the local microenvironment that surrounds a solute (i.e., the solute's cybotactic region) to a significant degree.[11−20] The effects of added water on solvent relaxation in a RTIL are, however, unknown. In this paper, we report new picosecond solvent relaxation results on PRODAN (chemical structure shown in Figure 1 inset) dissolved in dry [bmim][PF_6] and [bmim][PF_6] that contains 0.3, 0.8, 1.3, and 1.8 wt % water in the [bmim][PF_6] phase. The liquid−liquid equilibrium for water with [bmim][PF_6]at 298 K is ∼2.3 wt %;[40] hence, all experiments are performed below saturation.

Theory Section

The time evolution of a fluorescent solute's emission spectrum can be used to provide insights into how the cybotactic region relaxes/reorganizes around the excited-state fluorophore.[30−34,41,42] This solvent relaxation process can be studied by recording the fluorophore's time-resolved fluorescence intensity decay at several wavelengths across the emission profile.[41] In this work we have recorded the time-resolved intensity decay kinetics at 11 emission wavelengths across the PRODAN emission spectrum and we use these data to reconstruct the time-dependent emission center-of-gravity, $\nu(t)$,[41,42] the time-dependent emission spectral width, $\Delta\nu(t)$,[41] and the empirical solvent relaxation correlation function, $C(t)$.[42] $C(t)$ is often described in terms of an exponential series with time constants (τ_{ri}) and amplitudes (a_i)[30−34,41,42]

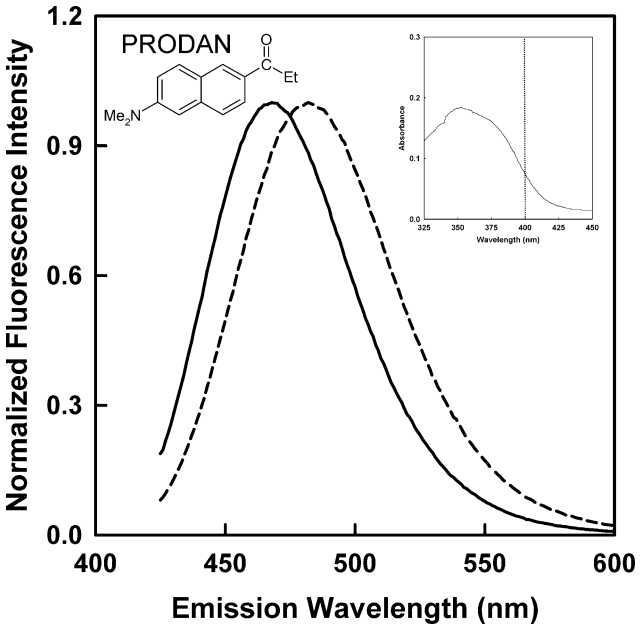

Figure 1. Steady-state emission spectra for PRODAN dissolved in dry (—) and wet (1.8 wt % water) (- - -) [bmim][PF_6] at 298 K. (Left inset) PRODAN chemical structure. (Right inset) PRODAN electronic absorbance spectra in [bmim][PF_6].

$$C(t) = [\nu(t) - \nu(\infty)]/[\nu(0) - \nu(\infty)] = \sum a_i \exp(-t/\tau_{ri}) \quad (1)$$

where the experimental measurables $\nu(t)$, $\nu(0)$, and $\nu(\infty)$ represent the emission center-of-gravities at times t, 0, and ∞, respectively. Of the three terms that one needs to compute $C(t)$, $\nu(0)$, the emission center-of-gravity that one would observe for a solute that has vibrationally relaxed *prior* to any solvent relaxation (i.e., a purely Franck−Condon state), is the most difficult to accurately determine.[42] (Note: Authors have used stretched exponentials and multiexponentials to represent $C(t)$;[21−26,30−34] however, theories are not available to justify either form over the other. In the current work we use the multiexponential representation.) In this work we estimate $\nu(0)$ from the steady-state PRODAN emission spectra in vitrified [bmim][PF_6] samples at 173 K (20 K *below* the [bmim][PF_6] glass transition temperature)[7] while exciting at the same wavelength that is used for the time-resolved studies (400 nm).

The overall solvent relaxation process can also be assessed by the average solvent relaxation time $\langle\tau_r\rangle$:[30−34,41,42]

$$\langle\tau_r\rangle = \sum(a_i\tau_{ri}) \quad (2)$$

Experimental Section

Reagents. Electrochemical-grade [bmim][PF_6] (stated 99+% pure; <50 ppm water; <50 ppm chloride; packaged under argon in Sure/SealJ bottles) was supplied

by Covalent Associates. PRODAN (Molecular Probes) and ethanol (Pharmco Products Inc., 200 proof) were used as received. All water was treated with a Barnstead NANOpure II system to a specific resistivity of >18 MΩ-cm. To avoid the undesired sorption of environmental moisture, all [bmim][PF_6] storage and sample preparation were performed under argon within a drybox.

Sample Preparation. To prepare a given PRODAN/[bmim][PF_6] sample, we micropipetted the appropriate volume of a PRODAN stock solution (in EtOH) into a series of clean, dry 1-cm^2 quartz cuvettes (Starna) equipped with a sealable cap and a stirring flea. The PRODAN concentration was ~10 μM. At this concentration, there was no evidence for PRODAN aggregation.[43] Residual EtOH was evaporated under gentle argon flow followed by a 30-min evacuation step (50 °C at 1 mbar). The desired amount of [bmim][PF_6] was then transferred into the cuvettes while they were kept within a drybox. All samples were then subjected to a 48 h vacuum step at 70 °C and 1 mbar to ensure water removal.[40,44]

The water-containing [bmim][PF_6] samples were prepared by maintaining the samples at 298 K and introducing water vapor by using a leak valve until a desired pressure was achieved.[40] The pressure was monitored by using a digital pressure gauge (Omega, model DPG10L-15G-HA-2LB) that was accurate to 0.1% between 0 and 1000 mbar. Samples were maintained at 298 K at a given pressure for at least 48 h with stirring to ensure the samples were at equilibrium. The solubility of water in each sample was determined from published water solubility vs P/P^{sat} isotherms at 298 K.[40] All experiments are performed below water saturation in the RTIL phase.

All samples were prepared in triplicate. The reported results are the average of all experiments. Imprecision is reported as ±1 standard deviation.

Spectroscopic Instrumentation. All steady-state fluorescence measurements were performed with an SLM-Aminco Model 48000 MHF spectrofluorometer (Spectronic Instruments). All spectra were background-corrected. The low-temperature spectra were recorded at 173 K by using our custom temperature stage.[45] The emission spectra for each sample remained constant for at least 2 weeks, if they were stored in the dark at room temperature.

The [bmim][PF_6] relaxation dynamics were studied by recording the PRODAN time-resolved intensity decay traces across the emission spectrum by using a laser/streak camera system. The laser consisted of a frequency-doubled femtosecond mode-locked Ti:sapphire laser (Coherent, Model Mira 900F) that was pumped by a cw Nd:vanadate laser (Coherent, Model Verdi). The laser output was tuned to 800 nm (400 nm after frequency doubling). The laser repetition rate was ~76 MHz, the pulse width was ~200 fs fwhm, and average laser power at the sample was 15−25 mW. The resulting PRODAN fluorescence was spectrally and temporally resolved by using a spectrograph−streak camera system (Hamamatsu Photonics K.K., Model C4334-11 Streakscope) that exhibited <15 ps temporal resolution and <20 ps jitter. The emission wavelength-dependent time-resolved intensity decay traces were fit independently to an exponential decay law (i.e., $I(t) = \sum \alpha_i \exp(-t/\tau_i)$) by using nonlinear least squares (Table Curve 2D v3) and $\nu(t)$, $\Delta\nu(t)$, and $C(t)$ generated as described elsewhere.[30−34,41,42]

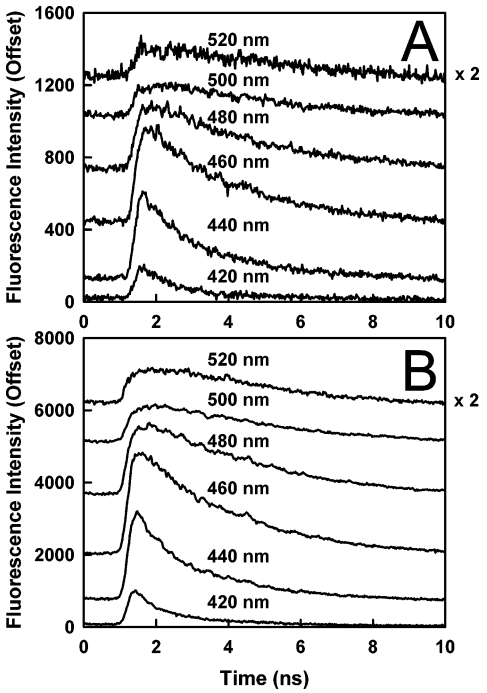

Figure 2. Representative wavelength-dependent time-resolved fluorescence intensity decay traces for PRODAN dissolved in [bmim][PF_6] at 298 K. (Panel A) Dry [bmim][PF_6]. (Panel B) [bmim][PF_6] with 1.8 ± 0.1 wt % water. The traces are off-set along the *y*-axis for clarity.

Results and Discussion

Figure 1 presents typical steady-state emission spectra for PRODAN (left inset) dissolved in [bmim][PF_6] at 298 K at two water loadings (dry, —, and 1.8 wt %, - - -). The corresponding electronic absorbance spectra are also shown (right inset). These spectra are similar to those seen for PRODAN dissolved in solvents such as liquid chloroform, DMF, acetone, glycerol, and ethanol.[13] These spectra show that an increase in the amount of solubilized water in the [bmim][PF_6] phase causes a substantial change in the *average* PRODAN cybotactic region. Specifically, PRODAN dissolved in dry [bmim][PF_6] encounters a microenvironment that lies between chloroform and DMF/acetone. In "wet" [bmim][PF_6], PRODAN encounters a microenvironment similar to an alcohol.

Figure 2 presents a typical series of raw PRODAN emission wavelength-dependent time-resolved fluorescence intensity decay traces in [bmim][PF_6] at 298 K at two water loadings. Parts A and B of Figure 2 present results for dry and wet (1.8 wt % water) samples, respectively. One can clearly see that the time-resolved intensity decays for both samples are characterized by a prompt emission in the blue portion of the spectrum that gives way, at the red edge, to decay traces that grow in with time and then decay away.

In Figure 3 we present typical time-resolved intensity decay traces (○) and fits (—) for PRODAN dissolved in [bmim][PF_6] at 298 K. These particular data were recorded for dry (Figure 3A,B) and wet (1.8 wt % water) samples (Figure 3C,D) while monitoring the emission at 430 nm (Figure 3A,C) and 490 nm (Figure 3B,D). There are three key features associated with these decay traces. First, the intensity decay data are always multiexponential at all emission wavelengths. Second, the red-edge emission (cf., Figure 3B,D) is always characterized by one apparent component with a nega-

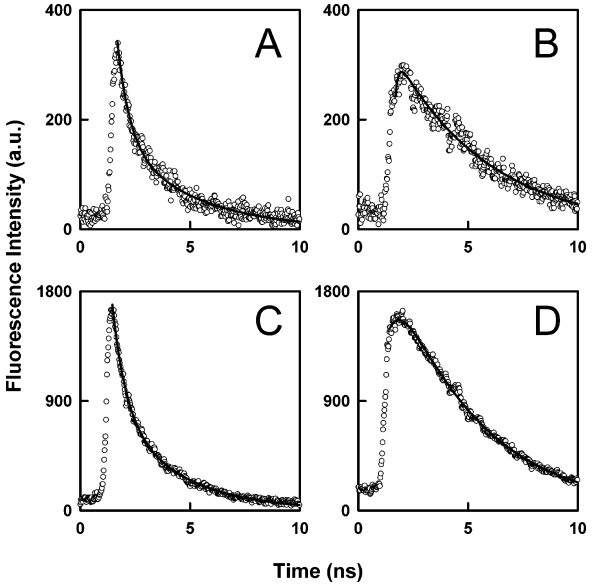

Figure 3. Typical time-resolved fluorescence intensity decay data (○) and corresponding fits (—) for PRODAN dissolved in [bmim][PF_6]. (Panel A) Dry [bmim][PF_6] at 430 nm. (Panel B) Dry [bmim][PF_6] at 490 nm. (Panel C) [bmim][PF_6] with 1.8 wt % water at 430 nm. (Panel D) [bmim][PF_6] with 1.8 wt % water at 490 nm.

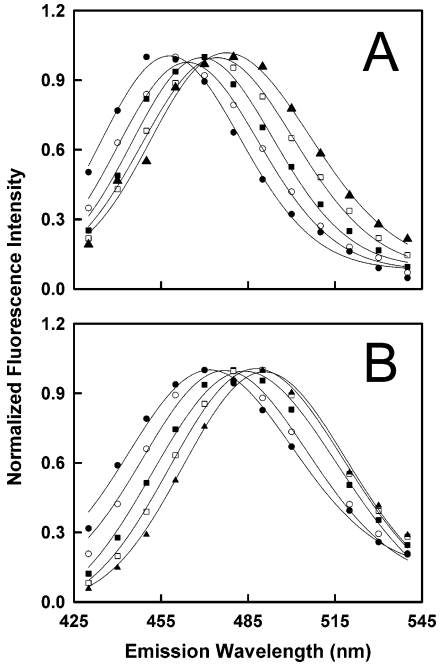

Figure 4. Typical time-resolved emission spectra (TRES) for PRODAN dissolved in [bmim][PF_6] at 298 K. (Panel A) Dry [bmim][PF_6]. (Panel B) [bmim][PF_6] with 1.8 ± 0.1 wt % water. At "0" (●), 0.5 (○), 2 (■), 6 (□), and 10 (▲) ns following optical excitation. The solid traces represent the best fits to a log-normal function.

tive pre-exponential term. Third, the decay kinetics are affected by the amount of solubilized water in [bmim][PF_6] phase.

From the time-resolved intensity decay parameters and the steady-state emission spectra, we can construct the time-resolved emission spectra (TRES).[41] Figure 4 presents a series of TRES for PRODAN dissolved in [bmim][PF_6] at 298 K at "0" (●), 0.5 (○), 2 (■), 6 (□), and 10 ns (▲) following optical excitation. These particular TRES are for dry (Figure 4A) and wet (1.8 wt % water) (Figure 4B) samples. The TRES shift to the red in a time-dependent manner for both samples, a characteristic of solvent relaxation. Inspection of these results also reveals that the magnitude and rate of this shift are a strong function of the amount of solubilized water in the [bmim][PF_6] phase. Specifically, at any given time following excitation, the PRODAN emission maximum from the [bmim][PF_6] sample that contains more water is always more red-shifted in comparison to the less wet sample, suggesting that PRODAN is emitting from a more relaxed state (on average) in the wetter [bmim][PF_6] samples. This result is consistent with the steady-state emission spectra (Figure 1).

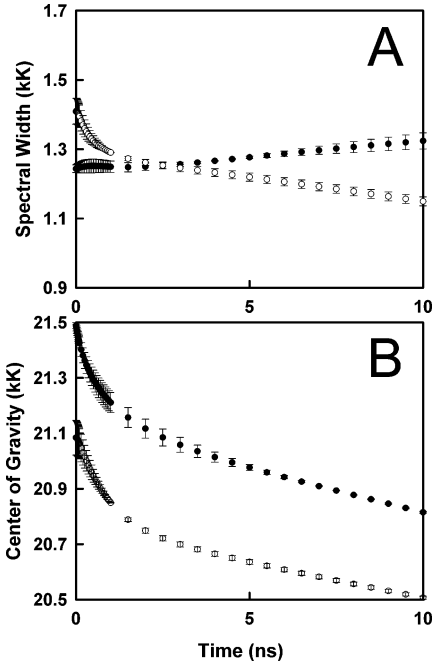

Figure 5. Summary of PRODAN transient solvation in dry (●) and wet (1.8 wt % water) (○) [bmim][PF_6] at 298 K. (Panel A) Average time-dependent spectral widths. (Panel B) Average time-dependent emission center-of-gravity. (1 kK = 10^3 cm^{-1}).

The TRES were used to construct the time-dependent emission spectral width and emission center-of-gravity.[40] Figure 5 presents average results for dry (●) and wet (1.8 wt % water) (○) samples. Figure 5A shows that the spectral width for the dry (●) sample remains essentially constant with time. This behavior is consistent with solvent relaxation occurring by a continuous relaxation process.[41] The time-dependent width results for [bmim][PF_6] that contains 1.8 wt % water (○) are not constant with time. At short times the spectra are broader than they are at longer times. One explanation for these results is that there are multiple microenvironments (e.g., water and [bmim][PF_6] rich) surrounding the PRODAN molecules in the wet samples. Figure 5B presents the time-resolved emission center-of-gravity for PRODAN dissolved in dry (●) and wet (1.8 wt % water) (○) [bmim][PF_6]. These results show that [bmim][PF_6] relaxation surrounding PRODAN occurs on nanosecond and sub-nanosecond time scales and there are substantial differences (vide infra) that depend on the amount of water solubilized in the [bmim][PF_6] phase.

To recover the true solvent relaxation kinetics (i.e., $C(t)$), we require an accurate estimate of $\nu(0)$. Toward this end, we recorded the steady-state PRODAN spectrum in dry (●) and wet (1.8 wt % water) (○) [bmim][PF_6] at 173 K (Figure 6). The recovered $\nu(0)$ values are 22800 ± 200 (●) and 22600 ± 200 cm^{-1} (○) for the dry and wet samples, respectively. In Figure 7 we present

Table 1. Recovered $C(t)$ Decay Parameters for PRODAN in [bmim][PF_6] at 298 K as a Function of Solubilized Water in the [bmim][PF_6] Phase

water content	a_{uf}[a]	τ_{uf} (ps)[a]	a_1	τ_{r1} (ns)	a_2	τ_{r2} (ns)	$\langle\tau_r\rangle$ (ns)[b]
<50 ppm	0.50 ± 0.04	<15	0.11 ± 0.03	0.59 ± 0.02	0.39 ± 0.01	16.34 ± 0.23	6.47 ± 0.20
0.3 wt %	0.56 ± 0.04	<15	0.10 ± 0.03	0.65 ± 0.04	0.34 ± 0.02	16.01± 0.35	5.52 ± 0.32
0.8 wt %	0.59 ± 0.03	<15	0.13 ± 0.04	0.75 ± 0.05	0.28 ± 0.01	15.93 ± 1.24	4.57 ± 0.55
1.3 wt %	0.61 ± 0.04	<15	0.12 ± 0.02	0.81 ± 0.10	0.27 ± 0.02	15.66 ± 1.47	4.33 ± 0.71
1.8 wt %	0.62 ± 0.05	<15	0.13 ± 0.02	0.87 ± 0.02	0.25 ± 0.01	15.24 ± 1.28	3.93 ± 0.63

[a] Component(s) that is (are) not resolved with our existing instrumentation ($a_{uf} + a_1 + a_2 = 1.00$). [b] $\langle\tau_r\rangle = \sum a_x\tau_x$.

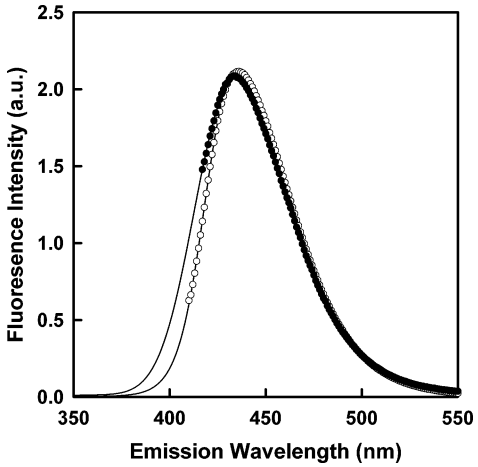

Figure 6. Steady-state emission spectra for PRODAN dissolved in dry (●) and wet (1.8 wt % water) (○) [bmim][PF_6] at 173 K. The solid lines are best fits to a log-normal function.

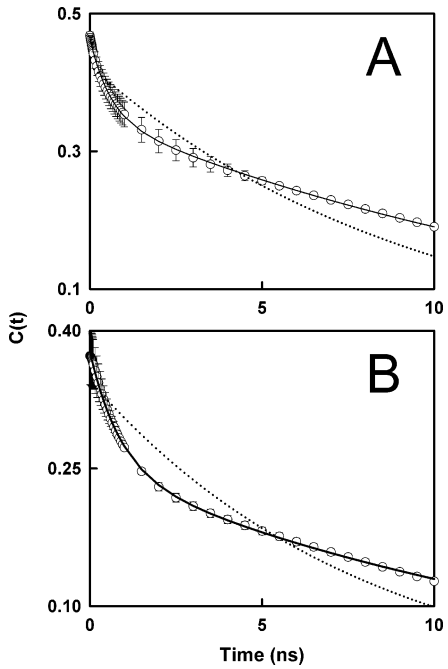

Figure 7. Recovered average $C(t)$ for PRODAN dissolved in [bmim][PF_6] at 298 K. (Panel A) Dry [bmim][PF_6]. (Panel B) [bmim][PF_6] with 1.8 ± 0.1 wt % water. Best fits (one component less than 15 ps) to double (- - -) and triple (—) exponential decay models.

the true $C(t)$ traces for PRODAN dissolved in dry (Figure 7A) and wet (1.8 wt % water) (Figure 7B) [bmim]-[PF_6] at 298 K along with fits to double (- - -) and triple (—) exponential models. (Note: One of the "apparent relaxation times" is <15 ps.) $C(t)$ is well-represented by a triple exponential model at all water levels. The recovered kinetic terms for $C(t)$ at all water loadings are collected in Table 1.

Inspection of Figure 7 and Table 1 show several interesting trends. First, the solvent relaxation dynamics within the local microenvironment that surrounds PRODAN in [bmim][PF_6] at 298 K occur over at least three time regimes. Second, our recovered $C(t)$ does not have a value of unity at time zero, as would be the case when all relaxation processes are recorded. Instead, between 50 and 62% (depending on water loading) of the total $C(t)$ relaxation occurs on a time scale that is faster than our 15-ps time resolution. Hence, the contribution from the sub-15 ps relaxation process(es) dominates $C(t)$ and its contribution increases by ~15% as the wt % of solubilized water in the [bmim][PF_6] phase increases. Third, the average relaxation time, $\langle\tau_r\rangle$, decreases by >60% as the wt % of solubilized water in the [bmim][PF_6] phase increases. Fourth, the longest of the recovered relaxation times (τ_{r2}) decreases by 7% as the wt % of solubilized water in the [bmim][PF_6] phase increases. Fifth, the *observed* solvent relaxation is dominated by the nanosecond τ_{r2} term. Finally, the intermediate relaxation time (τ_{r1}) *increases* from 0.59 to 0.87 ns as the wt % of solubilized water in the [bmim]-[PF_6] phase increases.

The overall relaxation process that we observe for PRODAN dissolved in [bmim][PF_6] is consistent with earlier studies;[21−26] however, our recovered relaxation dynamics are 2−5 times slower than previous results. We do not have an explanation for this apparent discrepancy. The presence of sub-15 ps dynamics is consistent with previous transient solvation experiments,[21−26] recent molecular dynamics simulations,[28,29] and recent ultrafast optical heterodyne-detected Raman-induced Kerr effect spectroscopy experiments.[27]

We assign the unquantified sub-15 ps dynamics (i.e., τ_{uf}), which dominate $C(t)$, to one or more of the following processes: libration and vibration, ion ballistic motion, ion local basin exploration, and ion basin hopping, ion diffusion,[27−29] or ultrafast relaxation of water (or another small agent).[46] We assign the two quantifiable relaxation times (τ_{r1} and τ_{r2}) to anion and cation relaxation, respectively, with τ_{r1} and τ_{r2} also depending on the cation size.[21−25] Our logic for these assignments is 6-fold. First, experiments[26] and simulations[27,28] show dynamics, occurring on a wide time scale, below 15 ps. Second, molecular dynamics simulations on [bmim][PF_6] at 298 K showed[28] that the anion and cation rotational reorientation time constants were 29 ps and 4.3 ns. Third, one cannot remove all the water from [bmim]-[PF_6] (even more difficult for the [BF_4] salts),[7,44] the contribution from the sub-15 ps, ultrafast component increased as the wt % of solubilized water in the [bmim]-[PF_6] phase increases, and there is sub-picosecond solvent relaxation in pure water[46] and water within restricted environments (e.g., reverse micelles).[47,48] Fourth, there is a significant slowing of τ_{r1} as water is added. This result surprised us given that the bulk [bmim][PF_6] viscosity decreases by ca. 12% when we go from dry to water-saturated [bmim][PF_6].[7,49] We specu-

late that this slowing results from hydrogen-bonding between water and the mobile [PF_6] anion. This view is consistent with recent FT-IR studies by Kazarian and co-workers on the molecular state(s) of water in ionic liquids, including [bmim][PF_6].[38] These authors found that water, at the level studied in the current work, exists in a 1:2 H-bonded complexes of the type [PF_6]···HOH···[PF_6] with a H-bonding enthalpy of nearly 8 kJ/mol. These FT-IR results suggest why the anion motion is hindered in the wet [bmim][PF_6] because these [PF_6]···HOH···[PF_6] interactions must be broken for the [PF_6] anion to reorient. Fifth, Huppert, and co-workers showed[22,23] that the ratio of the pre-exponential terms in $C(t)$ are a function of the relative ratio of the anion-to-cation diameters (A/C). Specifically, in their studies of coumarin 153 dissolved in molten tetraalkylamonium perchlorate salts, the authors found that a_{fast}/a_{slow} decreased as the A/C decreased when the anion remained fixed (perchlorate). We see a corresponding trend here in that a_1/a_2 increases as we go from dry to wet [bmim][PF_6]. This result is consistent, given that cation size is not changing upon the addition of water, with an increase in the size of the "anion" relative to the cation on adding water (i.e., [PF_6]···HOH···[PF_6] formation). Finally, there is a small 7% decrease in τ_{r2} as we add water. Given our measurement precision (τ_{r2} is at least 4 times longer than the PRODAN mean excited-state fluorescence lifetime), this small change is consistent with the decrease in the bulk [bmim][PF_6] viscosity and the interaction of the [bmim] cation with PRODAN.[11,13,14,18,50,51]

Conclusions

The solvation dynamics of PRODAN dissolved in [bmim][PF_6] as a function of added water in the RTIL phase have been measured with 15 ps time resolution. The solvation dynamics occur over a much wider time window in comparison to that of normal liquids (e.g., <15 ps to several nanoseconds). Libration and vibration, ion ballistic motion, ion local basin exploration, and ion basin hopping, ion diffusion, and/or the ultrafast relaxation from water (or other small molecules/impurities) could account for the yet unquantified sub-15 ps dynamics. The second apparent relaxation time, which increases as we add water, is assigned to anion relaxation. The increase in the relaxation time on adding water is explained in terms of 1:2 hydrogen bonding between water and [PF_6] anion, thus hindering the anion's ability to reorient. The longer relaxation time is assigned to the cation. As water is added, this relaxation time shortens in proportion to the overall decrease in the solvent viscosity. The anion and cation relaxation times depend on one another.

Acknowledgment

This work was supported by the U.S. Department of Energy and the NSF IGERT program. We thank Bruce J. Berne, Eric B. Brauns, Edward J. Maginn, and Mark Maroncelli for helpful discussions.

Literature Cited

(1) Chauvin, Y.; Olivier-Bourbigou, H. Nonaqueous Ionic Liquids as Reaction Solvents. *CHEMTECH* **1995**, *25*, 26.

(2) Seddon, K. R. Room-Temperature Ionic liquids: Neoteric Solvents for Clean Catalysis. *Kinet. Catal.* **1996**, *37*, 693.

(3) Seddon, K. R. Ionic Liquids for Clean Technology. *J. Chem. Technol. Biotechnol.* **1997**, *68*, 351.

(4) Welton, T. Room-Temperature Ionic Liquids. Solvents for Synthesis and Catalysis. *Chem. Rev.* (Washington, DC) **1999**, *99*, 2071.

(5) Bradley, D.; Dyson, P.; Welton, T. Room-Temperature Ionic Liquids. *Chem. Rev.* (Deddington, UK) **2000**, *9*, 18.

(6) Marsh, K. N.; Deev, A.; Wu, A. C.-T.; Tran, E.; Klamt, A. Room-Temperature Ionic Liquids as Replacements for Conventional Solvents − A Review. *Kor. J. Chem. Eng.* **2002**, *19*, 357.

(7) Huddleston, J. G.; Rogers, R. D. Room-Temperature Ionic Liquids as Novel Media for 'Clean' Liquid−Liquid Extraction. *Chem. Commun.* **1998**, 1765.

(8) Freemantle, M. Ionic Liquids Show Promise for Clean Separation Technology. *Chem. Eng. News* **1998**, *76*, 32.

(9) Spear, S. K.; Visser, A. E.; Willauer, H. D.; Swatloski, R. P.; Griffin, S. T.; Huddleston, J. G.; Rogers, R. D. Green Separation Science and Technology: Replacement of Volatile Organic Compounds in Industrial Scale Liquid−Liquid or Chromatographic Separations. In *ACS Symposium Series*; Anastas, P. T., Heine, L. G., Williamson, T. C., Eds.; American Chemical Society: Washington, DC, 2000; Vol. 766, p 206.

(10) The following companies are representative of vendors that sell a wide range of RTILs: Acros, Covalent Associates Inc., Merck, Scionix, and Solvent Innovation GmbH.

(11) Bonhôte, P.; Dias, A. P.; Papageorgiou, N.; Kalyanasundaram, K.; Grätzel, M. Hydrophobic, Highly Conductive Ambient-Temperature Molten Salts. *Inorg. Chem.* **1996**, *35*, 1168.

(12) Seddon, K. R. Electronic Absorption Spectroscopy in Room-Temperature Ionic Liquids. In *Molten Salt Chemistry: An Introduction and Selected Applications*; Mamantov, G., Marassi, R., Eds.; NATO ASI Series Vol. 202, Kluwer Academic Publishers B.V.: The Netherlands, 1987; p 365.

(13) Baker, S. N.; Baker, G. A.; Kane, M. A.; Bright, F. V. The Cybotactic Region Surrounding Fluorescent Probes Dissolved in 1-Butyl-3-methylimidazolium Hexafluorophosphate: Effects of Temperature and Added Carbon Dioxide. *J. Phys. Chem. B* **2001**, *105*, 9663.

(14) Baker, S. N.; Baker, G. A.; Bright, F. V. Temperature-Dependent Microscopic Solvent Properties of 'Dry' and 'Wet' 1-Butyl-3-methylimidazolium Hexafluorophosphate: Correlation with $E_T(30)$ and Kamlet−Taft Polarity Scales. *Green Chem.* **2002**, *2*, 165.

(15) Fletcher, K. A.; Storey, I. A.; Hemdricks, A. E. Pandey, S. Behavior of the Solvatochromic Probes Reichardt's Dye, Pyrene, Dansylamide, Nile Red and 1-Pyrenecarbaldehyde within the Room-Temperature Ionic Liquid [bmim][PF_6]. *Green Chem.* **2001**, *3*, 210.

(16) Fletcher, K. A.; Pandey, S. Effect of Water on the Solvatochromic Probe Behavior within Room-Temperature Ionic Liquid 1-Butyl-3-methylimidazolium Hexafluorophosphate. *Appl. Spectrosc.* **2002**, *56*, 266.

(17) Fletcher, K. A.; Pandey, S.; Storey, I. A.; Hendricks, A. E.; Pandey, S. Selective Fluorescence Quenching of Polycyclic Aromatic Hydrocarbons by Nitromethane within Room-Temperature Ionic Liquid 1-butyl-3-methylimidazolium Hexafluorophosphate. *Anal. Chim. Acta* **2002**, *453*, 89.

(18) Muldoon, M. J.; Gordon, C. M.; Dunkin, I. R. Investigations of Solvent−Solute Interactions in Room-Temperature Ionic Liquids Using Solvatochromic Dyes. *J. Chem. Soc.-Perkin Trans. 2* **2001**, 433.

(19) Aki, S. N. V. K.; Brennecke, J. F.; Samanta, A. How Polar are Room-Temperature Ionic Liquids? *Chem. Commun.* **2001**, 413.

(20) Lu, J.; Liotta, C. L.; Eckert, C. A. Spectroscopically Probing Microscopic Solvent Properties of Room-Temperature Ionic Liquids with the Addition of Carbon Dioxide. *J. Phys. Chem. A* **2003**, *107*, 3995.

(21) Bart, E.; Meltsin, A.; Huppert, D. Static and Dynamic Solvation Measurements of Excited Large Dipole in Molten Salt. *Chem. Phys. Lett.* **1992**, *200*, 592.

(22) Bart, E.; Meltsin, A.; Huppert, D. Solvation Dynamics of Coumarin 153 in Molten Salts. *J. Phys. Chem.* **1994**, *98*, 3295.

(23) Bart, E.; Meltsin, A.; Huppert, D. Solvation Dynamics in Molten Salts. *J. Phys. Chem.* **1994**, *98*, 10819.

(24) Karmakar, R.; Samanta, A. Solvation Dynamics of Coumarin-153 in a Room-Temperature Ionic Liquid. *J. Phys. Chem. A.* **2002**, *106*, 4447.

(25) Karmakar, R.; Samanta, A. Steady-State and Time-Resolved Fluorescence Behavior of C153 and PRODAN in Room-Temperature Ionic Liquids. *J. Phys. Chem. A* **2002**, *106*, 6670.

(26) Ingram, J. A.; Moog, R. S.; Ito, N.; Biswas, R.; Maroncelli, M. Solute Rotation and Solvation Dynamics in a Room-Temperature Ionic Liquid. *J. Phys. Chem. B* **2003**, *107*, 5926.

(27) Hyun, B.-R.; Dzyuba, S. V.; Bartsch, R. A.; Quitevis, E. L. Intermolecular Dynamics of Room-Temperature Ionic Liquids: Femtosecond Optical Kerr Effect Measurements on 1-Alkyl-3-methylimidazolium Bis((trifluoromethyl)sulfonyl)imides. *J. Phys. Chem. A* **2002**, *106*, 7579.

(28) Margulis, C. J.; Stern, H. A.; Berne, B. J. Computer Simulation of a "Green Chemistry" Room-Temperature Ionic Solvent. *J. Phys. Chem. B* **2002**, *106*, 12017.

(29) Morrow, T. I.; Maginn, E. J. Molecular Dynamics Study of the Ionic Liquid 1-*n*-Butyl-3-methylimidazolium Hexafluorophosphate. *J. Phys. Chem. B* **2002**, *106*, 12807.

(30) Simon, J. D. Time-Resolved Studies of Solvation in Polar Media. *Acc. Chem. Res.* **1988**, *21*, 128.

(31) Castner, E. W.; Bagchi, B.; Maroncelli, M.; Webb, S. P.; Ruggiero, A. J.; Fleming, G. R. The Dynamics of Polar Solvation. *Ber. Bunsen-Ges. Phys. Chem.* **1988**, *92*, 363.

(32) Maroncelli, M.; MacInnis, J.; Fleming, G. R. Polar Solvent Dynamics and Electron-Transfer Reactions. *Science* **1989**, *243*, 1674.

(33) Maroncelli, M. The Dynamics of Solvation in Polar Liquids. *J. Mol. Liq.* **1993**, *57*, 1.

(34) Bhattacharyya, K. Study of Organized Media Using Time-Resolved Fluorescence Spectroscopy. *J. Fluoresc.* **2001**, *11*, 167 and references therein.

(35) Seddon, K. R.; Stark, A.; Torres, M. J. Influence of Chloride, Water, and Organic Solvents on the Physical Properties of Ionic Liquids. *Pure Appl. Chem.* **2000**, *72*, 2275.

(36) Huddleston, J. G.; Visser, A. E.; Reichert, W. M.; Willauer, H. D.; Broker, G. A.; Rogers, R. D. Characterization and Comparison of Hydrophilic and Hydrophobic Room-Temperature Ionic Liquids Incorporating the Imidazolium Cation. *Green Chem.* **2001**, *3*, 156.

(37) Noda, A.; Hayamizu, K.; Wantanabe, M. Pulsed-Gradient Spin−Echo 1H and 19F NMR Ionic Diffusion Coefficient, Viscosity, and Ionic Conductivity of Non-Chloroaluminate Room-Temperature Ionic Liquids. *J. Phys. Chem. B* **2001**, *105*, 4603.

(38) Cammarata, L.; Kazarian, S. G.; Salter, P. A.; Welton, T. Molecular States of Water in Room Temperature Ionic Liquids. *Phys. Chem. Chem. Phys.* **2001**, *3*, 5192.

(39) Wong, D. S. H.; Chen, J. P.; Chang, J. M. Chou, C. H. Phase Equilibria of Water and Ionic Liquids [emim][PF_6] and [bmim][PF_6]. *Fluid Phase Equilib.* **2002**, *1194*, 1089.

(40) Anthony, J. L.; Maginn, E. J.; Brennecke, J. F. Solution Thermodynamics of Imidazolium-Based Ionic Liquids and Water. *J. Phys. Chem. B* **2001**, *105*, 10942.

(41) Lakowicz, J. R. *Principles of Fluorescence Spectroscopy*, 2nd ed.; Kluwer Academic/Plenum Publishers: New York, 1999; Chapter 7 and references therein.

(42) Fee, R. S.; Maroncelli, M. Estimating the Time-Zero Spectrum in Time-Resolved Emission Measurements of Solvation Dynamics. *Chem. Phys.* **1994**, *183*, 235.

(43) Sun, S. Y.; Heitz, M. P.; Perez, S. A.; Cólon, L. A.; Bruckenstein, S.; Bright, F. V. 6-Propionyl-2-(N,N-dimethylamino)naphthalene (PRODAN) Revisited. *Appl. Spectrosc.* **1997**, *51*, 1316.

(44) Tran, C. D.; Lacerda, S. H. D.; Oliveira, D. Absorption of Water by Room-Temperature Ionic Liquids: Effect of Anions on Concentration and State of Water. *Appl. Spectrosc.* **2003**, *57*, 152.

(45) Baker, S. N.; Baker, G. A.; Munson, C. A.; Bright, F. V. New Hot/Cold Stage for Performing Microfluorometric Measurements Continuously Between −120 and +100 °C. *Appl. Spectrosc.* **2001**, *55*, 1273.

(46) Jimenez, R.; Fleming, G. R.; Kumar, P. V.; Maroncelli, M. Femtosecond Solvation Dynamics of Water. *Nature* **1994**, *369*, 471.

(47) Zhang, J.; Bright, F. V. Nanosecond Reorganization of Water within the Interior of Reversed Micelles Revealed by Frequency-Domain Fluorescence Spectroscopy. *J. Phys. Chem.* **1991**, *95*, 7900.

(48) Riter, R. E.; Willard, D. M.; Levinger, N. E. Water Immobilization at Surfactant Interfaces in Reverse Micelles. *J. Phys. Chem. B* **1998**, *102*, 2705.

(49) Hamill, N. A.; Seddon, K. R.; Stark, A.; Torres, M. J. Viscosity and Density of 1-Alkyl-3-methylimidazolium Ionic Liquids. Presented at the American Chemical Society Meeting, Washington, April 2001; Paper IEC 279.

(50) Gordon, C. M.; McLean, A. J. Photoelectron Transfer from Excited-State Ruthenium(II) Tris(bipyridyl) to Methylviologen in an Ionic Liquid. *Chem. Commun.* **2000**, 1395.

(51) Schroder, U.; Wadhawan, J. D.; Compton, R. G.; Marken, R. Suarez, P. A. Z.; Consorti, C. S.; de Souza, R. F.; Dupont, J. Water-Induced Accelerated Ion Diffusion: Voltammetric Studies in 1-Methyl-3-[2,6-(S)-dimethylocten-2-yl]imidazolium Tetrafluoroborate, 1-Butyl-3-methylimidazolium Tetrafluoroborate and Hexafluorophosphate Ionic Liquids. *New J. Chem.* **2000**, *24*, 1009.

Received for review April 25, 2003
Revised manuscript received June 30, 2003
Accepted July 2, 2003

IE0303606